

Luminescence-intensity kinetics due to nonradiative capture by multiphonon emission in highly excited CdS and CdSe crystals

S. Juršėnas, G. Kurilčik, and A. Žukauskas*

Institute of Materials Science and Applied Research, Vilnius University, Naugarduko 24, 2006 Vilnius, Lithuania

(Received 17 June 1996)

The temporal kinetics of radiative recombination of a nonthermalized electron-hole plasma photoexcited by a powerful pulse of picosecond duration is considered with respect to the nonradiative capture of hot nonequilibrium carriers by deep centers via multiphonon emission (MPE). For centers thermally activated through surmounting the localization barrier by the carrier-lattice system, a decrease of the luminescence rise time and an occurrence of the fast-relaxation stage are shown to be characteristic of the band-to-band emission evolution at elevated lattice temperatures. An effect of MPE capture on the luminescence kinetics is experimentally demonstrated in CdS crystals with different concentrations of excess cadmium, and in a high-purity CdSe crystal. The analysis of the kinetics revealed deep traps, probably of native origin, with localization barriers of 110 meV for CdS and 215 meV for CdSe. [S0163-1829(96)00747-3]

I. INTRODUCTION

The luminescence kinetics in highly excited direct-gap semiconductors was extensively studied over the past few decades. In group II-VI compounds, routes of radiative recombination due to formation of excitons, biexcitons, and electron-hole plasma (EHP), stimulated emission, and collective interactions¹⁻¹¹ have been traced in the picosecond time domain. At high excitation, the carrier and exciton system is usually brought out of thermal equilibrium with the lattice, the relaxation of the relevant effective temperatures occurring on the nearly same time scale ($\sim 10-100$ ps) (Refs. 12-14) as the recombination.¹⁰ This makes an analysis of the recombination kinetics complicated, especially in the initial stages of the temporal evolution. Unfortunately, the experimental data are usually described by simplified kinetic models⁵⁻⁸ neglecting the dependence of recombination constants on effective temperature. The neglect is valid only for some special cases, e.g., at late stages of relaxation when the thermalization process is terminated. A nearly constant nonradiative recombination lifetime is also a good low-temperature approximation (see below). Meanwhile, at room temperature, important for potential applications, considering the luminescence kinetics in terms of simplified free-carrier recombination models^{6,8} becomes scarcely applicable because of the increased role of the effective-temperature-dependent nonradiative process. A more detailed investigation of luminescence kinetics with this process can provide additional information about nonradiative recombination routes, that are of crucial importance for the operation of electronic, optoelectronic, and optic devices. An example of such importance is the effect of thermally activated nonradiative recombination on the operation of an externally pumped semiconductor laser.¹⁵

An intrinsic nonradiative recombination route is the Auger process.¹⁶ However, in wide-band-gap semiconductors such as most group II-VI crystals, the Auger process is inefficient, and nonradiative recombination is due to the presence of deep levels acting in several ways. At low temperature,

excited states of certain centers can result in capturing the carriers by a cascade phonon emission.¹⁷ Additionally, for localized carriers, tunneling to nonradiative centers in real space¹⁸ may take place. Meanwhile, a delocalized carrier coupled with the lattice can be directly captured by a deep level by surmounting a certain localization barrier W caused by deformation of the lattice in the vicinity of the defect.¹⁹⁻²⁶ At low temperature, the barrier being too high, the carrier can be localized at the deep level via thermostimulated tunneling of the carrier-lattice system through the barrier in configuration space.^{20,23,24} The tunneling probability depends weakly on temperature, thus yielding a nearly constant nonradiative lifetime. At high temperatures, the energy of the carrier-lattice system can be sufficient to produce a lattice displacement equal to that around the defect. Under such conditions, a crossover of the free-electron-hole pair configuration potential curve with that of the deep level can be reached, resulting in a capturing of the carrier with a subsequent relaxation of the highly excited carrier-center system by multiphonon emission (MPE).^{20-22,24,25} In a semiclassical approach ($W \gg \hbar\omega$, where ω is the characteristic frequency of the phonon participating in the capture), a ground-state carrier-lattice system is localized at a capture center by MPE with the Arrhenius probability²¹

$$w \propto T^{-1/2} \exp(-W/k_B T), \quad (1)$$

where T is the equilibrium temperature. The validity of Eq. (1) is restricted to a temperature region that, for different estimations, ranges from²⁵ $T \gg \hbar\omega/2k_B$ to²⁴ $T \gg \hbar\omega/6k_B$. For instance, in CdS, assuming the energy $\hbar\omega$ is close to that of the LO phonon (38 meV), an exponential temperature dependence of the capture probability is thus expected for $T \gg 70-220$ K. The latter condition is difficult to reach conveniently in experiments (e.g., deep-level transient spectroscopy), as lattice temperatures above 400 K are typical for starting annealing processes in group II-VI crystals. This means that the value of W is unlikely to be determined from the temperature dependence of the capture cross section under equilibrium conditions.²⁵ For this reason poor data on the height

of the localization barrier, which is an important parameter for a lot of applications, are available.

Recently, we introduced a method of determining the barrier energy for nonequilibrium-carrier capture by MPE.²⁷ The method is based on the photoexcitation of quasithermalized electron-hole plasma with the carrier effective temperature elevated high above the room temperature (≈ 1000 K), and employs the sensitivity of the luminescence-intensity kinetics on the picosecond time domain to the barrier height. In the present work, extended data on the luminescence kinetics influenced by the MPE capture in group II-VI crystals (CdS and CdSe) are reported.

II. MODEL

The intensity kinetics of the luminescence due to radiative recombination in EHP is generally determined by the temporal evolution of the carrier density n and the effective temperature T_c . The transient luminescence intensity integrated over the spectrum is proportional to the spontaneous band-to-band recombination rate

$$I_{\text{LUM}} \propto R_{\text{sp}} = \frac{2\pi}{\hbar} \sum_{\mathbf{k}_e} \sum_{\mathbf{k}_h} |H_{\mathbf{k}_e \mathbf{k}_h}|^2 f_e(\mathbf{k}_e) f_h(\mathbf{k}_h) \times \delta(E_e(\mathbf{k}_e) + E_h(\mathbf{k}_h) + \bar{E}_g - h\nu), \quad (2)$$

where $|H_{\mathbf{k}_e \mathbf{k}_h}|^2$ is the square of the transition matrix element; $f_e(\mathbf{k}_e)$ and $f_h(\mathbf{k}_h)$ are the distribution functions of electrons and holes; $E_e(\mathbf{k}_e)$, $E_h(\mathbf{k}_h)$, \bar{E}_g , and $h\nu$ are the energies of the electron, hole, renormalized band gap, and emitted photon, respectively. Assuming the distribution functions to be Maxwell-Boltzmann ($f \propto n/T_c^{3/2}$), the band-to-band recombination rate can be expressed in terms of the bimolecular recombination coefficient γ

$$I_{\text{LUM}} \propto R_{\text{sp}} = \gamma(T_c(t)) n^2(t). \quad (3)$$

In the limit of strict validity of the \mathbf{k} -selection rule (direct transitions: $\mathbf{k}_e \approx \mathbf{k}_h$), the matrix element is almost constant, and the effective-temperature dependence of the bimolecular recombination coefficient as obtained from Eq. (2), is

$$\gamma(T_c) \propto T_c^{-3/2} \quad \text{or} \quad \gamma(T_c) = \gamma(T)(T/T_c)^{3/2}, \quad (4)$$

where $\gamma(T)$ is the coefficient at the equilibrium temperature. In dense plasma, the \mathbf{k} -selection rule may be weakened because of many-body interaction.^{28,29} In the limit of the full breakdown of the \mathbf{k} -selection rule, summation of the right-hand side of Eq. (2) must be performed over all possible pairs of \mathbf{k}_e and \mathbf{k}_h . Using a simplest form of the relevant square of the matrix element²⁸ $|H'_{\mathbf{k}_e \mathbf{k}_h}|^2 \propto |H_{\mathbf{k}_e \mathbf{k}_h}|^2 V^{-1}$, this yields the effective-temperature independent bimolecular coefficient

$$\gamma(T_c) = \gamma' \equiv \text{const.} \quad (5)$$

In nondegenerated plasma, the electron-hole pair density follows a rate equation comprising recombination terms in form of a power series

$$\frac{dn}{dt} = G(t) - \frac{n}{\tau(T_c(t))} - \gamma(T_c(t)) n^2 - C_A(T_c(t)) n^3 - \dots, \quad (6)$$

where τ and C_A are the effective-temperature-dependent carrier lifetime and the Auger coefficient (the Auger recombination and higher recombination terms can be neglected in wide-band-gap semiconductors). $G(t)$ is the carrier volume photogeneration rate that, for laser-pulse excitation, is usually of a Gaussian form

$$G(t) = I_L(\beta/\pi)^{1/2} \exp[-\beta(t/\tau_L)^2] / h\nu_L d, \quad (7)$$

where d is the thickness of the excited region, $\beta = 4 \ln(2)$, and I_L , τ_L , and $h\nu_L$ are the power density, the full width at half magnitude, and the photon energy of the exciting pulse. It should be noted that at high excitation power the exciting light penetrates the sample deeper than in the case of usual absorption ($\sim 0.1 \mu\text{m}$).^{14,30} This is due to filling the electron states responsible for incident photon absorption which are not able to deplete within the electron-electron and electron-phonon relaxation time (~ 10 fs). For incident photon flux power densities of the order 100 MW/cm^2 , the penetration depth is $\sim 1 \mu\text{m}$, while in group-II-VI crystals the drift length of nonequilibrium carriers is less than $1 \mu\text{m}$ at room temperature.³¹ This makes it possible to neglect the diffusion process in Eq. (6).

The carrier lifetime τ is generally contributed by all possible routes of recombination caused by imperfections of the crystal. It should be noted that, in our high-temperature case, the relative contribution of the thermostimulated tunneling in configuration space and the efficiency of the cascade phonon emission are vanishing, while the model of real-space tunneling is hardly applicable for plasma as a system of delocalized carriers. In addition the carrier density is considered to be high enough to saturate recombination routes involving band-to-level optical transitions. Thus, at high excitation and elevated temperatures, the carrier lifetime is to be predominantly determined by nonradiative capture via MPE. Below we assume that the capture is due to one dominant type of center, and generally is assisted by the nonequilibrium long-wavelength bulk LO-phonon modes occurring at high excitation.^{11,12,14} Meanwhile, the relaxation of the center with a captured carrier may produce a nonequilibrium occupation of the local vibration modes,³² which may affect the capture rate. However, in pure-component crystals, that are under consideration here, the capture is predominantly due to native defects such as vacancies which are known to modify the phonon density of states locally rather than to cause local vibration modes.³³ Thus, the MPE process is expected to produce some nonequilibrium LO phonons in addition to those excited by free-carrier cooling and second-generation nonequilibrium phonon fusion.^{14,30,34} Eventually, the long-wavelength bulk LO-phonon modes being brought out of thermal equilibrium with the crystal lattice because of relaxation of both free and localized carriers, the average occupation numbers N are close to those determined by the carrier effective temperature^{14,30} T_c as $N = [\exp(\hbar\omega/k_B T_c) - 1]^{-1}$. Averaging of the capture probability (1) over the nonequilibrium Maxwell-Boltzmann distribution must be performed in a way similar to that in Ref. 24. Finally, in the high-

temperature limit of the semiclassical approach, the effective-temperature dependence of the carrier lifetime is

$$\tau(T_c) \propto T_c^{3/2} \exp(W/k_B T_c). \quad (8)$$

At high excitation, the temporal behavior of the effective temperature $T_c(t)$ is determined by complex and mutually related energy-transfer processes in a system of hot plasma, localized carriers, and a few generations of nonequilibrium phonons. Below, for simplicity, we shall employ experimentally determined dependences $T_c(t)$.

The rate equation for the carrier density now can be rewritten with a glance at Eqs. (4), (5), (7), and (8),

$$\begin{aligned} \frac{dn}{dt} = & \frac{I_L}{h\nu_L d} \left(\frac{\beta}{\pi} \right)^{1/2} \exp \left[-\beta \left(\frac{t}{\tau_L} \right)^2 \right] \\ & - \frac{n}{\tau(T)} \left(\frac{T}{T_c(t)} \right)^{3/2} \exp \left[\frac{W}{k_B T} \left(1 - \frac{T}{T_c(t)} \right) \right] - \gamma(T_c) n^2, \end{aligned} \quad (9)$$

where $\tau(T)$ is the lifetime at the equilibrium temperature. In the limit of validity of the \mathbf{k} -selection rule, the bimolecular recombination coefficient $\gamma(T_c)$ is described by Eq. (4), while, if the \mathbf{k} -selection rule is broken, Eq. (5) is to be used.

It is worth noting that the recombination of an electron-hole pair via capture by MPE occurs in two steps each characterized by certain lifetimes of electron and hole capture, $\tau_e(T_c)$ and $\tau_h(T_c)$, respectively. Generally, the localization barriers for an electron (W_e) and a hole (W_h) being different, the pair lifetime is

$$\begin{aligned} \tau(T_c) = & \tau_e(T_c) + \tau_h(T_c) \\ = & \left(\frac{T_c}{T} \right)^{3/2} \left[\tau_e(T) \exp \left(\frac{W_e}{k_B T_c} \right) + \tau_h(T) \exp \left(\frac{W_h}{k_B T_c} \right) \right]. \end{aligned} \quad (10)$$

However, for $W_e \neq W_h$, the effective-temperature dependence of the sum lifetime is predominantly determined by the higher barrier of two. Here the lifetime $\tau(T_c)$ is considered to be independent of carrier density, i.e., we assume that, both types of carriers being present in the crystal, the relaxation of a center by MPE is fast enough to prevent the recombination from saturation.

In group II-VI crystals, typical room-temperature values of τ and γ are 10^{-9} s and 10^{-10} cm³/s, respectively. This makes the last term on the right-hand side of Eq. (9) negligible for carrier densities below 10^{19} cm³ and $T_c \geq T$. In this case, Eq. (9) becomes almost linear with respect to n , and at a fixed value of $\tau(T)$ the temporal evolution of the carrier density in relative units and, hence, the luminescence kinetics, depends mostly on the localization barrier height and on the kinetics of the effective temperature.

Typical temporal profiles of the radiative recombination in nonthermalized plasma calculated using Eqs. (3) and (9) for a few values of W in a CdS crystal with $\tau(T) = 1000$ ps are demonstrated in Fig. 1. The calculation was performed for the experimental situation of Ref. 14: the kinetics of the effective temperature [Fig. 1(a)] with a peak value $T_c^{\max} = 870$ K was used for $I_L = 100$ MW/cm², $h\nu_L = 3.50$ eV, and $\tau_L = 28$ ps. Three types of the luminescence kinetics can be

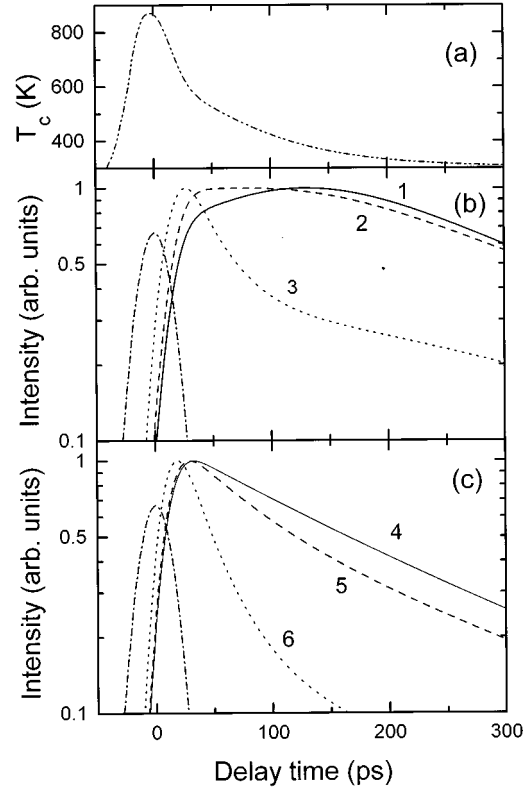


FIG. 1. Calculated luminescence kinetics in a highly excited CdS crystal. (a) Experimental effective-temperature dependence used in calculations. (b) Normalized kinetics in the case of validity of the \mathbf{k} -selection rule. (c) Same in the case of a breakdown of the \mathbf{k} -selection rule, no barrier ($W=0$); dashed lines, a “moderate” barrier ($W=100$ meV); dotted lines, a “high” barrier ($W=200$ meV); dash-dotted lines, the laser pulse.

distinguished in the case of the validity of the \mathbf{k} -selection rule (effective-temperature-dependent bimolecular recombination). For zero barrier ($W=0$, curve 1), the lifetime is almost constant, and the kinetics exhibits a phase of rise and a phase of exponential decay with a time constant $\tau(T)/2$. The rise is simultaneous with the stage of the heating relaxation, and is caused mainly by an increase of the radiative recombination rate with decreasing effective temperature [see Eq. (4)]. For a moderate barrier ($W \approx k_B T_c^{\max}$, curve 2), the rise time decreases as the increase of the radiative bimolecular recombination rate with decreasing the effective temperature is compensated for by a steeper dependence of the nonradiative recombination rate on the effective temperature. For high barrier ($W > k_B T_c^{\max}$, curve 3), this dependence produces a phase of rapid decrease of the luminescence intensity at the initial stage of the relaxation. The \mathbf{k} -selection rule being broken [Fig. 1(c)], the bimolecular recombination rate does not depend on the effective temperature, and the luminescence rise time is less pronounced for zero barrier, as this is determined only by an increase of the carrier density (curve 4). Therefore, the luminescence kinetics is less sensitive to the barrier height for $W \leq k_B T_c^{\max}$ on the relative scale of intensity (see curve 5 for $W \approx k_B T_c^{\max}$). Again, at $W > k_B T_c^{\max}$ (curve 6), a fast-relaxation phase occurs as in the case of the \mathbf{k} -selection rule, and the luminescence kinetics becomes sensitive to the barrier height. Generally, the local-

ization barrier can manifest itself in the kinetics of the radiative recombination of nonthermalized electron-hole plasma in two ways: by a reduction of the luminescence rise time for a “moderate” barrier height (type-I kinetics) and, additionally, by the occurrence of a stage of fast decay for a “high” barrier (type-II kinetics).

A prolonged rise time of the luminescence intensity due to effective-temperature-dependent bimolecular recombination was observed in CdSe at low temperature.¹⁰ In our recent short communication,²⁷ we demonstrated the possibility of determining a “moderate” barrier height in CdS crystals from the luminescence rise time, assuming the \mathbf{k} -selection rule is valid. Below, typical experimental kinetics of types I and II due to hot-carrier capture by MPE in group II-VI crystals (CdS and CdSe) are presented and analyzed in the limits of the validity and breakdown of the \mathbf{k} -selection rule.

III. EXPERIMENT AND RESULTS

In transient experiments, the samples were excited using a passively mode-locked YAG:Nd³⁺ (yttrium aluminum garnet) laser (the full width at half maximum pulse duration is $\tau_L=28$ ps, and the repetition rate is 2.7 Hz). The second harmonic of the laser irradiation ($h\nu_L=2.33$ eV) was used for excitation of CdSe crystals, and the third one ($h\nu_L=3.50$ eV) for CdS. The pump power densities were 200 and 100 MW/cm², respectively. The temporal resolution (≈ 30 ps) was provided by a CS₂ optical Kerr shutter. The luminescence spectra were dispersed by a 0.4-m grating monochromator and recorded photoelectrically by digital accumulation of the signal at each point, with discrimination of the laser pulses of unsuitable energy (the stability of the excitation intensity within 10% was preserved). The measurements were carried out at room temperature ($T=298$ K).

Type-I luminescence kinetics was found to be characteristic of CdS crystals with increasing enrichment by cadmium. CdS crystals grown from a high-purity vapor phase^{35,36} with different growth conditions were investigated. Here typical results for two samples are presented. Sample 1 was grown keeping the ratio of the partial pressures of cadmium and sulfur vapor components on the crystallization front $F=p(\text{Cd})/p(\text{S}_2)$ at the value of 0.64 that ensured the composition is almost stoichiometric. Sample 2 ($F=2.0$) was expected to have a higher concentration of native defects related with excess cadmium. Figure 2 presents low-temperature luminescence spectra of the samples excited by means of a cw He-Cd laser. The spectrum of sample 1 (solid line in Fig. 2) contains bound-exciton peaks related to shallow acceptors (I_{1A} at 2.536 eV) and donors (I_{2A} and I_{2B} around 2.547 eV) typical of undoped CdS crystals.^{37,38} A free-exciton polaritonic doublet (A_T and A_L) can be also resolved in the short-wavelength region. Sample 2, grown with increased partial pressure of cadmium (dotted line in Fig. 2), is seen to exhibit an I_{2C} line near 2.545 eV characteristic of CdS crystals with sulfur vacancies³⁸ V_S and a long-wavelength shifted I_{1B} line at 2.535 eV.

Figure 3 presents some time-resolved luminescence spectra of a highly excited sample 2 at room temperature for a few values of delay after the peak of the excitation pulse. The spectra are seen to contain one emission band which can be attributed to radiative recombination of dense EHP.^{4,14,31}

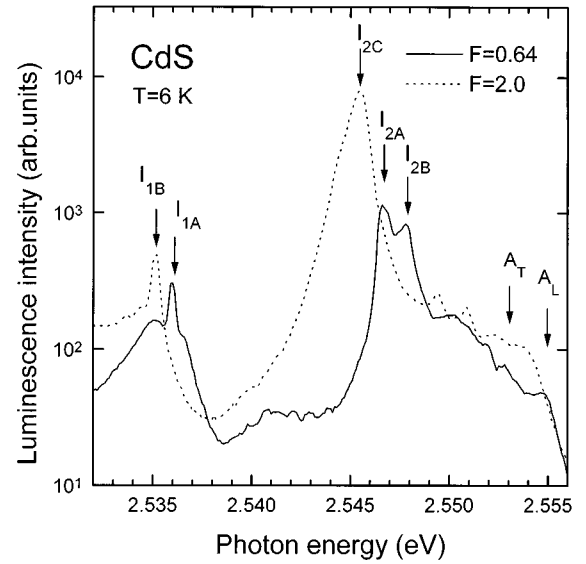


FIG. 2. Low-temperature luminescence spectra of two CdS crystals for cw excitation.

The high-energy region of the spectra was used to determine the carrier effective temperature by fitting the experimental shape with the theoretical ones. The fitting was performed for two models of radiative recombination: with and without \mathbf{k} -selection rule taken into account.²⁹ The suitability of each model was tested by bringing the obtained T_c values close to the equilibrium value T at large delay time. Figure 4(a) shows the obtained $T_c(t)$ dependences for sample 2 (for sample 1 the dependences are almost the same). The \mathbf{k} -selection rule being taken into account [diamonds in Fig.

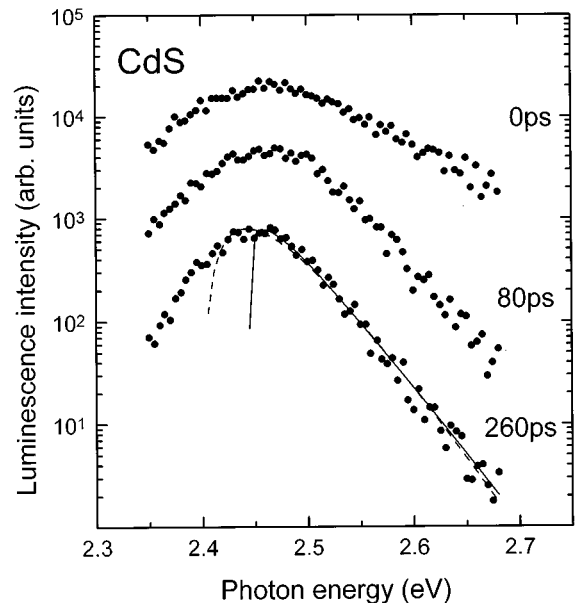


FIG. 3. Transient luminescence spectra of a CdS crystal (sample 2). The spectra are arbitrarily shifted along the vertical axis, and the delay time after the exciting pulse is indicated at each spectrum. Solid line, an example of approximation of the high-energy wing by a calculated line shape with the \mathbf{k} -selection rule taken into account ($T_c=301$ K); dashed line, same neglecting the rule ($T_c=250$ K).

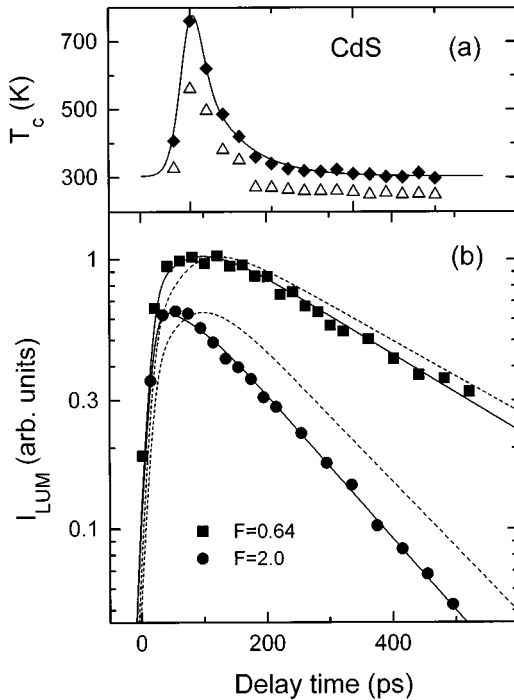


FIG. 4. (a) Temporal evolution of the carrier effective temperature in CdS crystals. Diamonds show values obtained from line shapes regarding the \mathbf{k} -selection rule; triangles, the same with the rule disregarded; solid line, the approximation used in calculations. (b) Transient behavior of the integral luminescence intensity for two CdS crystals. Points, experiment; solid lines, calculation for $W=110$ meV. The dashed lines, reproducing the calculation for $W=0$, are shifted along the vertical axis to normalize the peak intensities.

4(a)], the effective temperature is seen to reach a value of ≈ 770 K at zero delay, and to relax exactly to the equilibrium value soon after terminating the excitation pulse. It should be noted that the spectral position of the luminescence band indicates a negligible increase in the lattice temperature, the obtained effective temperature T_c referring only to plasma and the phonon modes involved in the primary stages of the energy relaxation.¹⁴ Disregard of the \mathbf{k} -selection rule [triangles in Fig. 4(a)] yields a $T_c(t)$ dependence that drops below the equilibrium temperature at large delay time. Thus luminescence kinetics should be analyzed only with the \mathbf{k} -selection rule taken into consideration, i.e., with an effective-temperature-dependent radiative bimolecular recombination rate as given by Eq. (4).

Points in Fig. 4(b) depict the variation of the luminescence intensity integrated over the spectrum with time in two samples. In comparison with sample 1, sample 2 is seen to exhibit not only a lower emission efficiency and a smaller decay time τ_{LUM} for the late-stage luminescence kinetics (185 ps vs 380 ps), but also a shorter rise time. To estimate the localization barrier height, both experimental luminescence kinetics were fitted with those calculated using Eqs. (3) and (9). It should be noted that the electron-hole pair density estimated from the bandwidth does not exceed $5 \times 10^{18} \text{ cm}^{-3}$, which makes the model of a nondegenerated plasma applicable. Calculations employ an approximation of the experimental dependence $T_c(t)$ [solid line in Fig. 4(a)]

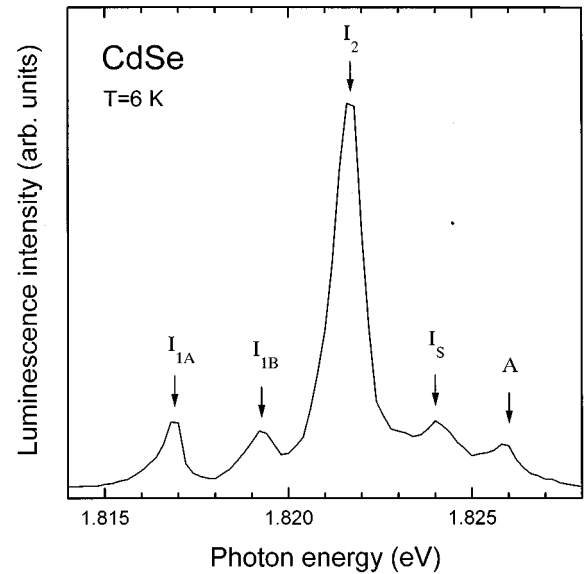


FIG. 5. Low-temperature luminescence spectrum of a CdSe crystal for cw excitation.

and experimental values of $\tau(T) = 2\tau_{\text{LUM}}$ (760 and 370 ps for samples 1 and 2, respectively). Using the equilibrium value of the bimolecular recombination coefficient³⁹ $\gamma(T) = 1.4 \times 10^{-10} \text{ cm}^3/\text{s}$, the calculated kinetics was insensitive to the thickness of the excited region d in the range above $5 \mu\text{m}$, and the fit was achieved by varying only the one parameter W . Solid lines in Fig. 4(b) show the result of the best fit achieved for $W=110$ meV ($d=5 \mu\text{m}$). Dashed lines depict the solution for $W=0$. One can see that the experimental data cannot be reasonably described without an introduction of nonradiative recombination thermally activated through a nonzero barrier W . The zero barrier yields a prolonged rise time for both samples.

A characteristic type-II luminescence kinetics was observed in a CdSe crystal grown from the high-purity vapor phase. Figure 5 shows a luminescence spectrum in the excitonic region recorded at $T=6$ K under low cw excitation by He-Cd laser irradiation. In the short-wavelength part, the spectrum exhibits pronounced intrinsic peaks of the free (A at 1.826 eV) (Ref. 40) and surface mechanic (I_S at 1.824 eV) (Ref. 41) excitons. At lower energies bound-exciton peaks (I_{1A} at 1.817 eV, I_{1B} at 1.819 eV, and I_2 at 1.822 eV), related with shallow donors and acceptors (probably Cd_i and Se_i interstitials),^{40,42} dominate. The spectrum is typical of a high-purity CdSe crystal predominantly comprising “native” defects.⁴⁰

Time-resolved luminescence spectra due to radiative recombination of EHP (Refs. 2, 3, and 10) are depicted in Fig. 6. Contrary to the case of CdS, the high-energy region of the spectra fits the line shape better with the \mathbf{k} -selection rule neglected,²⁹ as follows from the values of the effective temperature obtained for large delay times. Figure 7(a) shows the obtained temporal evolution of the carrier effective temperature with a peak value of ≈ 780 K at zero delay and relaxation to the equilibrium value T within ~ 100 ps. In the case when the \mathbf{k} -selection rule is taken into account, no relaxation to the equilibrium value of the temperature is achieved. Thus a further analysis of the luminescence kinet-

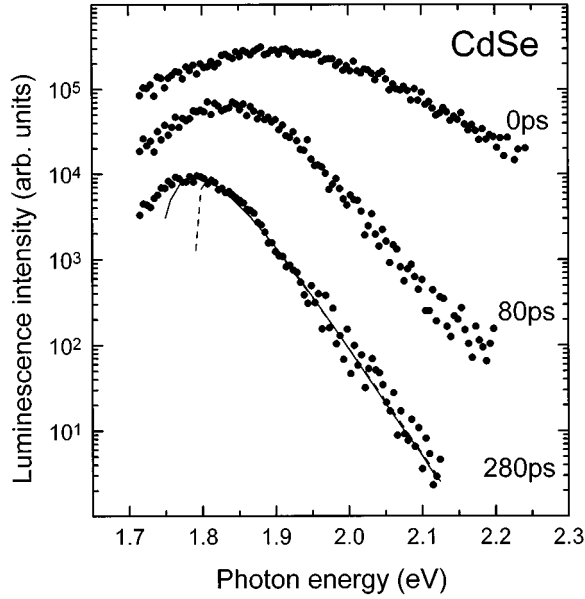


FIG. 6. Transient luminescence spectra of a CdSe crystal. The spectra are arbitrarily shifted along the vertical axis, and the delay time after the exciting pulse is indicated at each spectrum. Solid line, an approximation with neglect of the \mathbf{k} -selection rule ($T_c = 317$ K); dashed line, same with the rule taken into account ($T_c = 391$ K).

ics should be performed with the \mathbf{k} -selection rule neglected. The contrast in validity of the \mathbf{k} -selection rule between CdSe and CdS crystals is probably caused by the large difference in hole mass, the lighter holes in CdSe contributing more to many-body processes than those heavier in CdS.

Points in Fig. 7(b) depict the temporal variation of the luminescence intensity integrated over the spectrum (the low-energy wing of the spectra, that could not be measured because of the limited operation spectrum of the Kerr shutter, was approximated assuming a symmetric line shape of the plasma band). The plasma being hot, the luminescence kinetics is seen to exhibit a short rise time with a subsequent fast-relaxation phase. The thermal relaxation being terminated, the kinetics takes the form of a slow exponential decay with a time constant of $\tau_{\text{LUM}} = 600$ ps ($\tau = 2\tau_{\text{LUM}} = 1200$ ps). The observed evolution of the plasma recombination emission intensity can be attributed to the case of a “high” barrier, as it resembles curve 6 in Fig. 1(c). To obtain an exact value of W , fitting with the kinetics calculated in accordance with Eqs. (3) and (9) was performed with effective-temperature-independent bimolecular recombination coefficient [Eq. (5)]. Taking the values of $d > 10$ μm and $\gamma' < 10^{-10}$ cm^3/s , the MPE capture dominates in the recombination, and the fit can be achieved by varying only the one parameter W . The solid line in Fig. 7(b) depicts the result of the calculation for $W = 215$ meV ($d = 10$ μm and $\gamma' = 1 \times 10^{-10}$ cm^3/s). The dashed line shows the calculated kinetics for $W = 0$, that is seen to be very distant from the experimental one.

IV. DISCUSSION AND CONCLUSIONS

The origin of the centers of the nonradiative recombination in CdS ($W = 110$ meV) and CdSe ($W = 215$ meV) is to

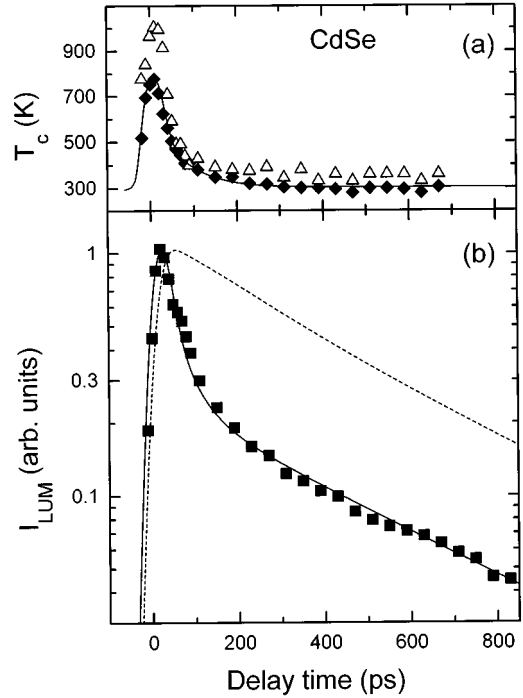


FIG. 7. (a) Temporal evolution of the carrier effective temperature in a CdSe crystal. Diamonds show values obtained from line shapes with the \mathbf{k} -selection rule disregarded; triangles, the same regarding the rule; solid line, the approximation used in calculations. (b) Transient behavior of the integral luminescence intensity. Points, experiment; solid line, calculation for $W = 215$ meV. The dashed line, reproducing the calculation for $W = 0$, is shifted along the vertical axis to normalize the peak intensity.

be discussed. In our crystals, produced from high-purity components, the most probable centers of MPE capture are deep “native” traps. The excitonic spectra (Figs. 2 and 5) imply the domination of shallow levels due to interstitials (e.g., Cd_i and Se_i in CdSe).⁴⁰ Hence the crystals should contain a lot of their Frenkel codefects in the form of vacancies. In CdSe, the vacancies V_{Cd} and V_{Se} are known to produce deep levels,^{43,44} moreover, cadmium vacancies were identified as centers of fast recombination⁴⁴ (s centers). Probably, a similar situation is typical of CdS crystals, where excess cadmium, as in the case of sample 2, is expected to produce sulfur vacancies.³⁸ Using a typical value for a cross section of a point defect²¹ $\sigma \sim 10^{-15}$ cm^2 , one can estimate the density of centers of MPE capture as $N = (\sigma v_T \tau)^{-1}$, where v_T is the thermal velocity of the carrier. At room temperature ($\tau \approx 1000$ ps), the estimated density N is around $10^{16} - 10^{17}$ cm^{-3} ; that is, typical of “native” point defects in group II-VI crystals.⁴⁵

The obtained values of the barrier height can be used to reconstruct the configuration diagrams of the centers of capture via MPE. Assuming these centers are vacancies producing no local vibration mode, a Huang-Rhys model,¹⁹ with the uniform vibration frequency for the lattice coupled with both free and localized carriers, should be employed.⁴⁶ An example of reconstruction for the center of nonradiative recombination in our CdS crystals was demonstrated in Ref. 27 using the data on the energy of photoactivation.⁴⁵ Figure 8 depicts a reconstructed configuration diagram of the deep

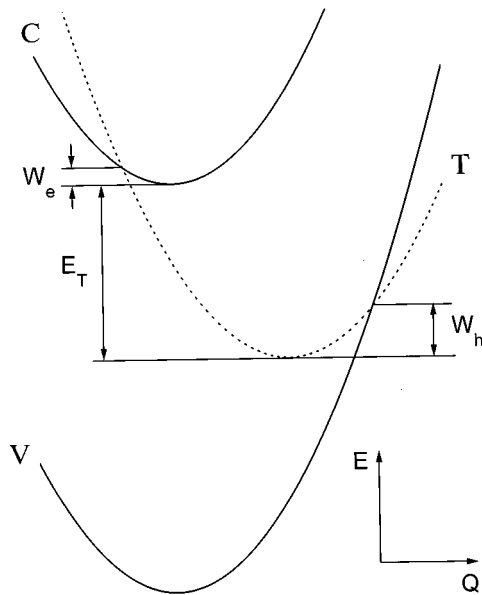


FIG. 8. Configuration diagram of a possible center of nonradiative recombination in CdSe.

level in CdSe located at $E_T=0.75$ eV below the bottom of the conduction band.⁴⁴ As the experimental data do not provide information about which type of carrier (electron or hole) the measured barrier is to be attributed to, the configuration curve of the center was selected from a few possible ones in a way that ensured that the barrier for the second carrier is much lower than that of the measured one (215 meV). Thus Fig. 8 reproduces the case of the high barrier for the hole ($W_h \approx W = 215$ meV), and a lower one for the electron ($W_e = 70$ meV $< W_h$). This implies a total recombination rate to be determined by MPE capture of holes rather than by that of electrons.

In conclusion, the temporal evolution of the hot electron-hole plasma radiative recombination was analyzed using a rate equation with a carrier-effective-temperature dependent lifetime in respect of the capture by MPE. The shape of the

luminescence intensity kinetics was shown to be strongly dependent on the height of the localization barrier. A typical manifestation of a “moderate” barrier as a reduction of the luminescence rise time was experimentally demonstrated for CdS and CdS:Cd crystals, while the effect of a “high” barrier, additionally producing the fast-relaxation stage, was observed in a CdSe crystal. Configuration diagrams of the centers of nonradiative recombination can be reconstructed using the values of the barrier height obtained by fitting the experimental luminescence intensity kinetics with the calculated ones. The dominating centers of capture by MPE in the investigated group II-VI crystals were supposed to originate from “native” point defects, probably vacancies.

Our results imply that, at elevated temperatures, in group II-VI crystals with intrinsic densities of native defects, the linear recombination channel prevails over the bimolecular recombination under conditions of high excitation by a laser pulse of picosecond duration. During the excitation pulse action, the increase of the MPE capture probability overcomes that of the radiative bimolecular recombination because of the high effective temperature. Consequently, the lifetime drops to tens of picoseconds, resulting in a nonradiative disappearance of the greater part of the initially excited carriers. Further, after the laser pulse is terminated, the remainder of the carrier density is too small to make bimolecular recombination important. However, bimolecular recombination still provides the principal mechanism of the radiative emission, though affecting the carrier density only weakly.

Providing that the capture by MPE at native centers excites LO vibrations in the long-wavelength region, a mechanism of plasma heating emerges due to absorption of the nonequilibrium phonons by free carriers. This mechanism should considerably increase the excess effective temperature during the laser-pulse action, and slow down the cooling after the pulse has been terminated.

ACKNOWLEDGMENTS

The work was supported by the Lithuanian State Science and Education Foundation (Grant No. 96-148/2F). We thank G. Tamulaitis for technical assistance and discussions.

*Electronic address: arturas.zukauskas@ff.vu.lt

¹M. Hayashi, H. Saito, and S. Shionoya, *Solid State Commun.* **24**, 833 (1977).

²H. Saito, M. Hayashi, and S. Shionoya, *Solid State Commun.* **24**, 837 (1977).

³T. Daly and H. Mahr, *Solid State Commun.* **25**, 323 (1978).

⁴H. Yoshida, H. Saito, S. Shionoya, and V. B. Timofeev, *Solid State Commun.* **33**, 161 (1980).

⁵A. Cornet, J. Collet, T. Amand, M. Pugno, B. S. Razbirin, and G. Michailov, *J. Phys. Chem. Solids* **44**, 53 (1983).

⁶V. A. Kovalenko, I. V. Kryukova, and S. P. Prokof'eva, *Kvant. Elektron. (Moscow)* **8**, 1790 (1981) [*Sov. J. Quantum Electron.* **11**, 1079 (1981)].

⁷H. Saito, *J. Lumin.* **30**, 303 (1985).

⁸V. S. Dneprovskii, V. I. Klimov, and M. G. Novikov, *Fiz. Tverd. Tela (Leningrad)* **30**, 2938 (1988) [*Sov. Phys. Solid State* **30**, 1694 (1988)].

⁹A. A. Klochikhin, B. S. Razbirin, D. K. Nelson, T. Amand, M.

Brousseau, J. Collet, A. Cornet, and M. Pugno, *Phys. Status Solidi B* **147**, 727 (1988).

¹⁰R. Baltramiejūnas, S. Juršenas, A. Žukauskas, E. Kuokštis, and V. Latinis, *Fiz. Teh. Poluprovodn.* **23**, 565 (1989) [*Sov. Phys. Semicond.* **23**, 353 (1989)].

¹¹J. H. Collet, W. W. Rühle, M. Pugno, K. Leo, and A. Million, *Phys. Rev. B* **40**, 12 296 (1989).

¹²W. Pötz and P. Kocevar, *Phys. Rev. B* **28**, 7040 (1983).

¹³J. Collet, M. Pugno, A. Cornet, M. Brousseau, B. S. Razbirin, and G. V. Mikhailov, *Phys. Status Solidi B* **103**, 367 (1981).

¹⁴S. Juršenas, A. Žukauskas, and R. Baltramiejūnas, *J. Phys. Condens. Matter* **4**, 9987 (1992).

¹⁵A. Žukauskas and I. V. Kryukova, *Kvant. Elektron. (Moscow)* **17**, 872 (1990) [*Sov. J. Quantum Electron.* **20**, 792 (1990)].

¹⁶P. T. Landsberg, *Phys. Status Solidi* **41**, 457 (1970).

¹⁷M. Lax, *Phys. Rev.* **119**, 1502 (1960).

¹⁸R. A. Street, *Adv. Phys.* **25**, 397 (1976).

- ¹⁹K. Huang and A. Rhys, Proc. R. Soc. London Ser. A **204**, 406 (1950).
- ²⁰R. Kubo and Y. Toyozawa, Prog. Theor. Phys. **13**, 160 (1955).
- ²¹C. H. Henry and D. V. Lang, Phys. Rev. B **15**, 989 (1977).
- ²²B. K. Ridley, J. Phys. C **11**, 2323 (1978).
- ²³V. N. Abakumov, I. A. Merkulov, V. I. Perel, and I. N. Yassievich, Zh. Eksp. Teor. Fiz. **89**, 1472 (1985) [Sov. Phys. JETP **62**, 853 (1985)].
- ²⁴A. S. Ioselevich and E. I. Rashba, Zh. Eksp. Teor. Fiz. **91**, 1917 (1986) [Sov. Phys. JETP **64**, 1137 (1986)].
- ²⁵D. Goguenheim and M. Lannoo, J. Appl. Phys. **68**, 1059 (1990).
- ²⁶J. H. Zheng, H. S. Tan, and S. C. Ng, J. Phys. Condens. Matter **6**, 1695 (1994).
- ²⁷A. Žukauskas and S. Juršėnas, Appl. Phys. Lett. **67**, 1095 (1995).
- ²⁸G. Lasher and F. Stern, Phys. Rev. **133**, A553 (1964).
- ²⁹Y. Yoshikuni, H. Saito, and S. Shionoya, Solid State Commun. **32**, 665 (1979).
- ³⁰A. Žukauskas and S. Juršėnas, Phys. Rev. B **51**, 4836 (1995).
- ³¹H.-E. Swoboda, M. Sence, F. A. Majumder, M. Rinker, J.-Y. Bigot, J. B. Grun, and C. Klingshirn, Phys. Rev. B **39**, 11 019 (1989).
- ³²V. A. Kovarskii, E. A. Popov, and I. A. Chaikovskii, Phys. Status Solidi B **67**, 427 (1975).
- ³³M. Lannoo and J. C. Bourgoin, *Point Defects in Semiconductors I, Theoretical Aspects*, edited by M. Cardona, Springer Series in Solid State Sciences Vol. 22 (Springer-Verlag, Berlin, 1981), Chap. 5.
- ³⁴V. Klimov, P. Haring Bolivar, and H. Kurtz, Phys. Rev. B **52**, 4728 (1995).
- ³⁵E. V. Markov and A. A. Davydov, Izv. Akad. Nauk SSSR Neorg. Mater. **11**, 1755 (1975) [Inorg. Mater. **11**, 1504 (1975)].
- ³⁶O. V. Bogdankevich, N. N. Kostin, E. M. Krasavina, I. V. Kryukova, E. V. Markov, E. V. Matveenko, and V. A. Teplitskii, Izv. Akad. Nauk SSSR Neorg. Mater. **23**, 1618 (1987) [Inorg. Mater. **23**, 1428 (1987)].
- ³⁷D. G. Thomas and J. J. Hopfield, Phys. Rev. **128**, 2135 (1962).
- ³⁸E. T. Handelman and D. G. Thomas, J. Phys. Chem. Solids **26**, 1261 (1965).
- ³⁹Y. P. Varshni, Phys. Status Solidi **19**, 459 (1967).
- ⁴⁰E. F. Gross, B. S. Razbirin, V. P. Fedorov, and Yu. P. Naumov, Phys. Status Solidi **30**, 485 (1968).
- ⁴¹A. S. Batyrev, B. V. Novikov, and A. E. Cherednichenko, Fiz. Tverd. Tela (Leningrad) **23**, 2982 (1981) [Sov. Phys. Solid State **23**, 1739 (1981)].
- ⁴²B. S. Razbirin and I. N. Uraltsev, Fiz. Tverd. Tela (Leningrad) **13**, 605 (1971) [Sov. Phys. Solid State **13**, 493 (1971)].
- ⁴³R. Baubinas, Z. Januškevičius, A. Sakalas, and J. Viščiakas, Solid State Commun. **15**, 1731 (1974).
- ⁴⁴A. Sakalas and R. Baubinas, Phys. Status Solidi A **31**, 301 (1975).
- ⁴⁵A. Kazlauskas, V. Gavryushin, G. Račiukaitis, and O. Makienko, J. Cryst. Growth **146**, 59 (1995).
- ⁴⁶V. N. Abakumov, V. I. Perel, and I. N. Yassievich, *Nonradiative Recombination in Semiconductors*, edited by V. M. Agranovich and A. A. Maradudin, Modern Problems in Condensed Matter Sciences Vol. 33 (North-Holland, Amsterdam, 1991), Chap. 9.